Available online at www.sciencedirect.com
ScienceDirect
International Journal of Heat and Mass Transfer 51 (2008) 3410–3419
International Journal of HEAT and MASS TRANSFER
www.elsevier.com/locate/ijhmt

Simulation of droplet spreading, splashing and solidification using smoothed particle hydrodynamics method

M.Y. Zhang [a], H. Zhang [b,c], L.L. Zheng [b,*]

[a] Institute of Applied Physics and Computational Mathematics, Beijing 100088, China
[b] Department of Mechanical Engineering, Stony Brook University, Stony Brook, NY 11794, USA
[c] Department of Engineering Physics, Tsinghua University, Beijing 100084, China

Received 4 May 2007; received in revised form 3 November 2007
Available online 27 December 2007

Abstract

Spreading, splashing and solidification of yttria stabilized zirconia (YSZ) droplet after inclined impact are simulated by smoothed particle hydrodynamics. The artificial heat model has been improved and a simple solidification model is included. It is found that the droplet splashes when the impact angle is less than 44° with the Reynolds number of 3535. Otherwise the droplet will deposit. The result is in good agreement with the theoretical prediction. The temperature distribution and solidification interface movement during the droplet impacting on an inclined surface are presented. The flattening ratio is found to increase with the impact angle.

Keywords: Droplet dynamics; Spreading; Solidification; Splashing; Smoothed particle hydrodynamics; Meshless method

1. Introduction

Thermal spray is a continuous, direct melt-spray process in which particles of virtually any material are melted and accelerated to high velocities. The molten or semi-molten droplets impact on a substrate and rapidly solidify to form thin "splats". The performance of the coating is intimately related to the shape of the splats and how they bond together and to the substrate. A droplet impacts the solid substrate surface, deforms and spreads to a so-called 'pancake' or 'exploded' shape. The final morphology of the splat depends on the droplet diameter, temperature, velocity, and melting status [1,2].

Experimental studies have focused on the impact of molten droplets on a smooth or rough substrate. Escure et al. [3] investigate the impact of liquid alumina droplets on different substrates. The Sommerfeld parameter was used to describe the impact behavior, such as rebound, deposition, and splashing. Šikalo et al. [4] studied the droplets impacting on a substrate with low impact angles and low normal Weber numbers. The effects of impact angle and viscosity on droplet impact behavior were provided. Kang and Ng [5] quantified the spreading behavior of individual splats at different substrate inclinations using the spread factor and aspect ratio. The fitted quadratic equations for spreading behavior were obtained. Xu et al. [6] used the high-speed photography to study the corona splashing due to the impact of a liquid drop on a smooth dry substrate. It was discovered that decreasing surrounding gas pressure inhibits splashing. The threshold pressure is a function of the impact velocity, molecular weight of the gas, and the liquid viscosity. It was concluded that the compressibility of the gas is responsible for splashing.

Numerical simulations were performed to investigate the important and complex phenomena during droplet impact in thermal spray coating. Zhang [7] proposed a theoretical model based on the volume of fluid (VOF) for droplet spreading and solidification considering surface tension, solidification and thermal contact resistance. The

* Corresponding author.
E-mail address: Lili.Zheng@sunysb.edu (L.L. Zheng).

0017-9310/$ - see front matter
doi:10.1016/j.ijheatmasstransfer.2007.11.009

Nomenclature

c_p	specific heat, J/kg K
d	droplet diameter, m
D	the effective diameter of the splat, m
f	force, N
h	smoothing length, m
H	artificial heat, J/kg s
I	unit tensor
k	thermal conductivity, W/m K
K	Sommerfeld number
L	latent heat, J/kg
m	particle mass, kg
p	pressure, Pa
Re	Reynolds number ($=\rho Vd/\mu$)
t	time, s
T	temperature, K
u	internal energy, J/kg
$\vec{v}$	particle velocity vector, m/s
V	velocity scale, m/s
W	smoothing function, m^{-3}
We	Weber number ($=\rho V^2 d/\sigma$)
x	particle position, m

Greek symbols

ε	constant related to the interaction between SPH particles
θ	impact angle
μ	viscosity coefficient, kg/m s
ξ	flattening ratio
ρ	particle density, kg/m^3
σ	surface tension, J/m^2
σ_r	characteristic distance, m
φ	Lennard-Jones potential, J
∇	gradient operator

Subscripts

$i\ j$	particle index
m	melting
l	liquid
p	particle or droplet
s	solid

splat-flattening ratio was described as a function of Reynolds, Weber, Prandtl and Jakob numbers. Zhang et al. [8] investigated the splat morphology and substrate melting and re-solidification numerically and experimentally and found that the droplet size, velocity, temperature, and substrate material and temperature all play the significant roles in splat morphology and rate of solidification. Zhang et al. [9] developed a splat formation model based on the classic nucleation theory, which considered heterogeneous nucleation kinetic and crystal growth. The model can predict the nucleation temperature and grain size distribution. Based on the scaling analysis, the nucleation delay and solidification times have been derived. Zhang and Zheng [10,11] developed a numerical model based on the level set method to study the droplet deformation and solidification in two and three dimensions. They simulated that the solidification interface movement and splat morphology for a molten droplet impacting on an inclined surface. Bussmann et al. [12] developed a three-dimensional model based on the VOF-based RIPPLE code where the surface tension force was simulated as a volume force and the measured contact angle was provided as the boundary condition for simulations. The oblique impact of a 2 mm water droplet at 1 m/s onto a 45° incline and the impact of a droplet onto a sharp edge were simulated. Numerical results were compared with the experimental pictures. Bussmann et al. [13] investigated the fingering and splashing of a droplet impacting on a solid surface. Simulation results for molten tin, water, and heptane droplets agreed with the experiments. Pasandideh-Fard et al. [14] extended the three-dimensional model developed by Bussmann et al. [12]. The enthalpy method was used to solve the solidification problem. The deposition of tin droplets on a stainless steel surface was investigated using both experiments and numerical simulations. Simulation results agreed well with the experimental pictures. Mostaghimi et al. [2] proved that the flattening ratio is related to the Reynolds number and, to a less degree, the Weber number, and splashing is resulted from the perturbation of solidification. However, the effect of solidification on droplet spreading can be neglected when the ratio of the Stefan number to the Prandtl number is much smaller than unity. Zhang et al. [15] applied the smoothed particle hydrodynamics (SPH) model to study the droplet impacting problem for the first time. Effects of substrate roughness and solidification on splat morphology were investigated. Oxide redistribution and droplet pinch-off were studied in two and three dimensions. Multiple droplets impacting on a flat substrate was also simulated. In their model, the surface tension force was not included and the heat transfer equation was not solved.

Extended from the previous work of Zhang et al. [15], this paper will present an improved SPH model by solving the energy equation using an improved artificial heat model. A simple solidification model is also included to simulate the movement of the solidification interface. The new model is used to study the effect of impact angle on droplet splashing under the traditional plasma spray conditions, e.g., high speed and small size of the droplet. The temperature distribution and solidification interface movement are presented. In the following, the numerical model will be presented first, followed by simulation results and discussions.

2. Numerical model

Smoothed particle hydrodynamics (SPH) is a meshless Lagrangian method for fluid dynamics simulation. As a particle method, SPH uses a set of particles to represent fluid flow. All the physical and mathematical properties of the fluid are assigned to the SPH particles. Mathematically, the particles are only the interpolation points. The properties of the fluid are calculated on these points.

The mass density ρ_i of the particle at the position $\vec{x}_i$ can be evaluated by using the summation density:

$$\rho_i(\vec{x}) = \sum_{j=1}^{N} m_j W_{ij}, \tag{1}$$

where $W_{ij} = W(\vec{x}_{ij}, h)$ is the smoothing function, and $\vec{x}_{ij} = \vec{x}_i - \vec{x}_j$, m_i denotes the mass of particle i, h represents the smoothing length and $\vec{x}_i$ is the position of particle i. By integrating Eq. (1), we obtain the total mass of the system which is equal to the summation of all the particles. The summation density has the property of mass conservation.

Applying the SPH particle approximation to the Lagrangian form of the Navier-Stokes equations, a symmetric form is obtained to preserve variational consistency. The momentum equation can be written as follows

$$\frac{\mathrm{D}\vec{v}_i}{\mathrm{D}t} = -\sum_{j=1}^{N} m_j \left(\frac{p_i}{\rho_i^2} + \frac{p_j}{\rho_j^2}\right)\nabla_i W_{ij} + \sum_{j=1}^{N} m_j \left(\frac{\tau_i}{\rho_i^2} + \frac{\tau_j}{\rho_j^2}\right)\cdot \nabla_i W_{ij} + \vec{f}. \tag{2}$$

The RHS of Eq. (2) consists of the pressure, viscous force and surface tension force. The particle approximation for the viscous stress tensor τ is

$$\tau_i = -\sum_{j=1}^{N} \frac{m_j}{\rho_j} \mu_i \vec{v}_{ij} \nabla_i W_{ij} - \sum_{j=1}^{N} \frac{m_j}{\rho_j} \mu_i (\nabla_i W_{ij}) \vec{v}_{ij} + \left(\frac{2}{3}\sum_{j=1}^{N} \frac{m_j}{\rho_j} \mu_i \vec{v}_{ij}\cdot \nabla_i W_{ij}\right) I. \tag{3}$$

Surface tension force plays a significant role in the droplet impact. The Lennard-Jones potential has been widely used to simulate the surface tension force, since the Lennard-Jones force is repulsive at the short distance and attractive at the long distance. The Lennard-Jones potential takes the form of the empirical function as follows [16]

$$\varphi(r) = 4\varepsilon\left[\left(\frac{\sigma_r}{r}\right)^{12} - \left(\frac{\sigma_r}{r}\right)^{6}\right], \tag{4}$$

where σ_r is a characteristic distance between the SPH particles and ε is a constant related to the interaction between SPH particles. Usually the characteristic distance σ_r takes the value of the initial inter-particle distance. According to the SPH particle approximation, the Lennard-Jones force takes the SPH form as follows

$$\vec{f}_i = -\nabla\varphi_i = -\sum_{j=1}^{N} \frac{m_j}{\rho_j} \varphi_j \cdot \nabla W_{ij}. \tag{5}$$

Fulk [17] proposed an artificial heat model to describe the heat conduction problem. The artificial heat model has the following form

$$H_i = 2\sum_{j=1}^{N} \frac{\bar{q}_{ij}}{\bar{\rho}_{ij}} \frac{u_i - u_j}{|x_{ij}|^2 + \varphi^2} \vec{x}_{ij}\cdot \nabla_i W_{ij}, \tag{6}$$

where

$$q_i = \alpha_{\Pi} h_i \rho_i c_i |\nabla\cdot \vec{v}_i| + \beta_{\Pi} h_i^2 \rho_i |\nabla \cdot \vec{v}_i|^2, \tag{7}$$

$$\bar{q}_{ij} = q_i + q_j, \tag{8}$$

$$\bar{\rho}_{ij} = \rho_i + \rho_j. \tag{9}$$

The artificial heat model is based on the difference of the internal energy. However, heat conduction/convection is related to the temperature difference. Usually the artificial heat model can handle the heat conduction/convection problem since there is a linear relationship between the internal energy and the temperature. However, for the problem with phase transform, the model based on the internal energy cannot describe the heat transfer correctly. Therefore, we modify the artificial heat model as follows

$$H_i' = 2\sum_{j=1}^{N} \frac{\bar{c}_{p_{ij}} \bar{q}_{ij}}{\bar{\rho}_{ij}} \frac{T_i - T_j}{|x_{ij}|^2 + \varphi^2} \vec{x}_{ij}\cdot \nabla_i W_{ij}, \tag{10}$$

$$\bar{c}_{p_{ij}} = (c_{p_i} + c_{p_j})/2, \tag{11}$$

where c_p is the specific heat of the particle. The modified model is based on the temperature difference and we will use this model to study the solidification problem.

Based on the modified artificial heat model, the energy equation can be rewritten as

$$\frac{Du_i}{Dt} = \frac{1}{2}\sum_{j=1}^{N} m_j \left(\frac{p_i}{\rho_i^2} + \frac{p_j}{\rho_j^2}\right)\vec{v}_{ij}\cdot \nabla_i W_{ij} - \frac{1}{2}\sum_{j=1}^{N} m_j \left(\frac{\tau_i}{\rho_i^2} + \frac{\tau_j}{\rho_j^2}\right) : \vec{v}_{ij} \nabla_i W_{ij} + H_i'. \tag{12}$$

In order to simulate the fluid flow with solidification, a simple solidification model is proposed here. According to the internal energy calculated by the above energy

Table 1
YSZ properties used in the modeling

Material	YSZ
k_s, W/m K	2.0
k_l, W/m K	2.32
$c_{p,s}$, J/kg K	580
$c_{p,l}$, J/kg K	713
ρ_s, kg/m^3	5890
ρ_l, kg/m^3	5890
T_m, K	2950
L, J/kg	7.07×10^5
μ, kg/m s	0.008

equation, the temperature can be obtained from the linear relationship between the temperature and the internal energy. The latent heat was taken into consideration. The status of the SPH particle can be specified by the following rule

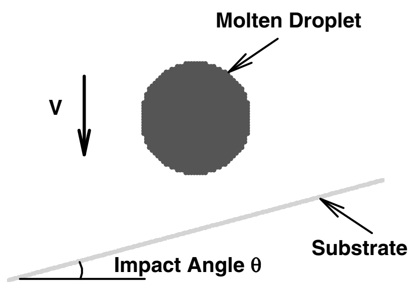

Fig. 1. Schematic of a molten droplet impacting on a cold substrate with an impact angle θ.

$$u\begin{cases} > c_pT_{\mathrm{m}} + L & \text{liquid,} \\ \text{between} & \text{melting,} \\ < c_pT_{\mathrm{m}} & \text{solid.} \end{cases} \tag{13}$$

where T_{m} is the melting temperature and L is the latent heat. Eq. (12) together with Eqs. (1) and (2) can be used to solve the flow and temperature fields, and solidification of the molten droplets impacting on an inclined surface. Noted that the solidification model proposal here is similar to the enthalpy method used in the meshed methods.

3. Results and discussion

To study the impact behavior of YSZ droplet onto the inclined substrate, numerical simulations have been performed using different impact angles. The YSZ properties used in simulations are listed in Table 1. Fig. 1 shows the schematic of droplet impacting on a cold substrate with

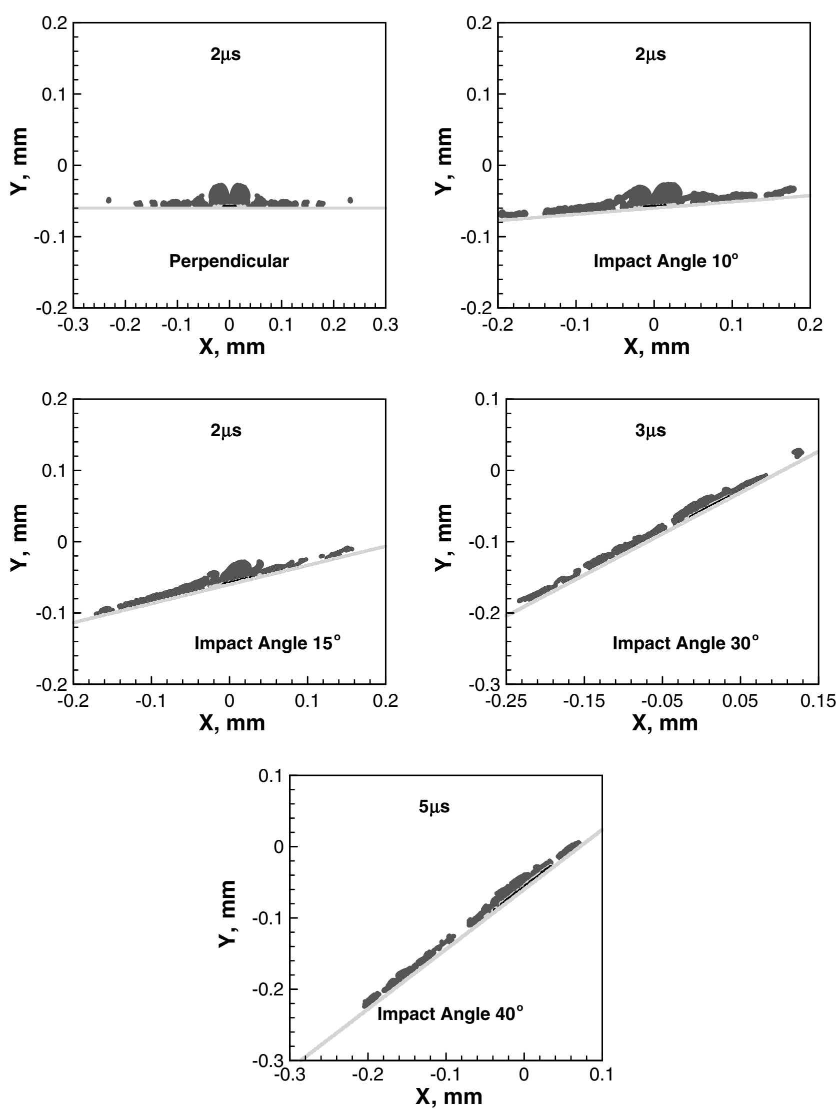

Fig. 2. YSZ droplet splashes at impact angles of 0°, 10°, 15°, 30°, and 40°, respectively. The dark gray color is liquid, the light gray color is the solidification interface, the dark color is solid, and the light gray line is substrate.

an impact angle θ. The initial diameter of the YSZ droplet is 60 μm, the impact velocity of the droplet is 80 m/s, and the impact angles are 0°, 10°, 15°, 30°, 40°, 45°, 60°, and 75°. Since the droplet size is very small, surface tension has a great influence on the splat formation. The Lennard-Jones force is used to model the surface tension. The SPH particles of equal mass have the uniform initial inter-particle distance of 1.5 μm or 3 μm, in 2D or 3D, respectively. The smoothing length is the same as the inter-particle distance. For the impact velocity of 80 m/s, the Reynolds number can be estimated as 3535. The initial temperature of the droplet is assumed to be 3000 K uniformly. The substrate temperature is set to be 500 K. Thermal contact resistance is not considered here. The time step in the simulations is 1 ns. The total number of particles used to represent a droplet in 2D or 3D is 1212 or 4224, respectively. The computer Dell Precision PWS690 with Xeon 3.20 GHz CPU is used in our simulations. The running time of 1000 time steps in 2D or 3D is about 300 s or 1200 s, respectively.

3.1. Droplet splashing

Depending on droplet parameter and substrate condition, the molten droplet will rebound, deposit, or splash. The ejection of tiny droplets in the impact direction is so-called impact splashing. This type of splashing is the result of the Rayleigh-Taylor instability when a molten droplet spreads into a less dense one [18]. Another type of splashing is called the flattening splashing. The flattening splashing occurs when solidification starts during the flattening process. The Sommerfeld number K is used to describe the splashing behavior, which is defined as

$$K = We^{1/2}Re^{1/4}, \tag{14}$$

where We and Re are the Weber and Reynolds numbers, respectively, defined with the normal velocity component of the droplet as follows:

$$We = \frac{\rho\, \mathrm{d}V^2 \cos^2\theta}{\sigma}, \tag{15}$$

$$Re = \frac{\rho\, \mathrm{d}V \cos\theta}{\mu}. \tag{16}$$

According to the experiments [3,19–21], at least for a water or a ethanol droplet, K is the criterion that can be used to judge the splashing behavior. The criterion is described below

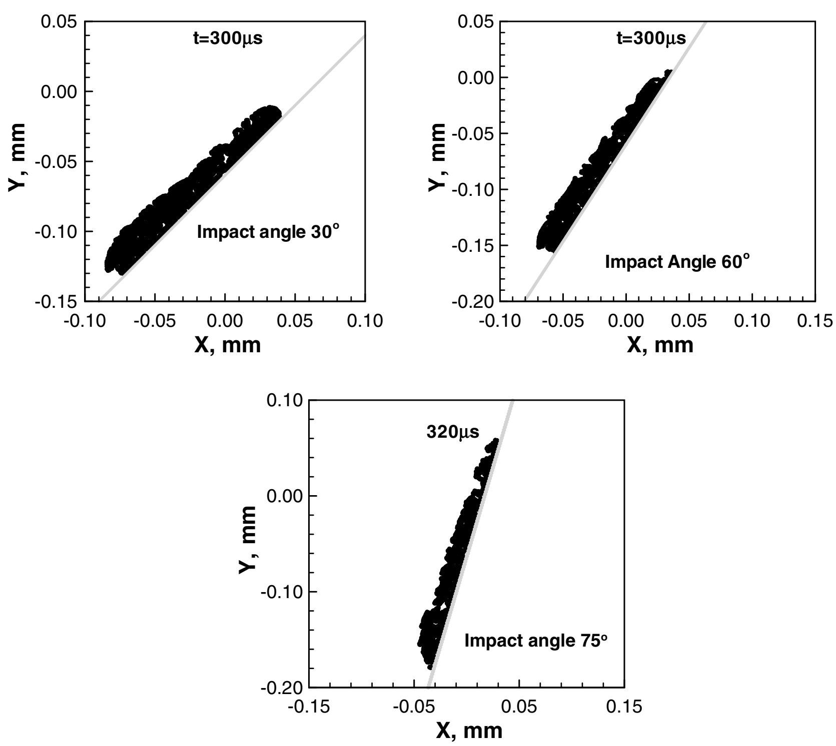

Fig. 3. YSZ droplet deposits at impact angles of 45°, 60°, and 75°, respectively. The dark gray color is liquid, the light gray color is the solidification interface, the dark color is solid, and the light gray line is substrate.

Table 2
Splashing behavior at $Re = 3535$ and impact angles of 0°, 10°, 15°, 30°, 40°, 45°, 60°, and 75° with initial temperature of 3000 K

Impact angle	0°	10°	15°	30°	40°	45°	60°	75°
Impact behavior	Splash	Splash	Splash	Splash	Splash	Deposition	Deposition	Deposition

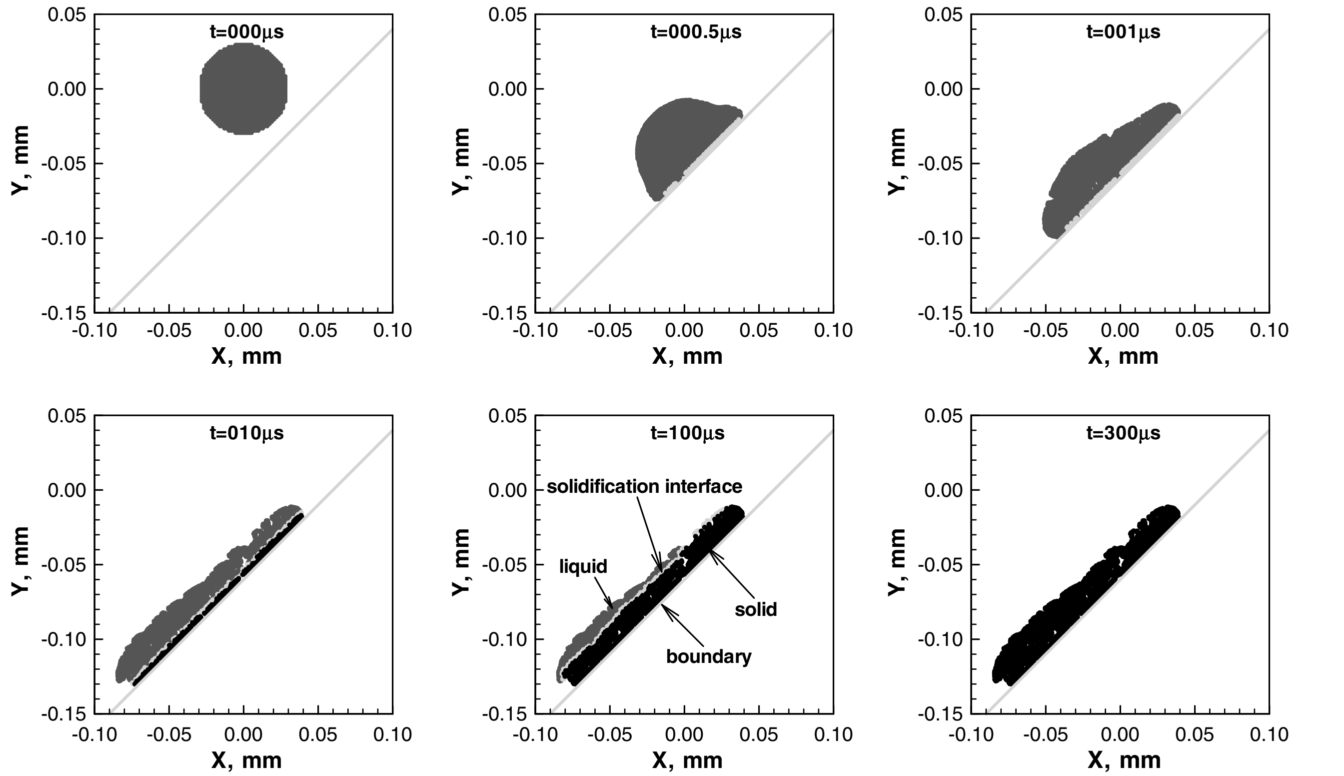

Fig. 4. Droplet impacts on a cold substrate in 2D for $Re = 3535$ and impact angle of 45° with initial temperature of 3000 K. The dark gray color is liquid, the light gray color is the solidification interface, the dark color is solid, and the light gray color line is substrate.

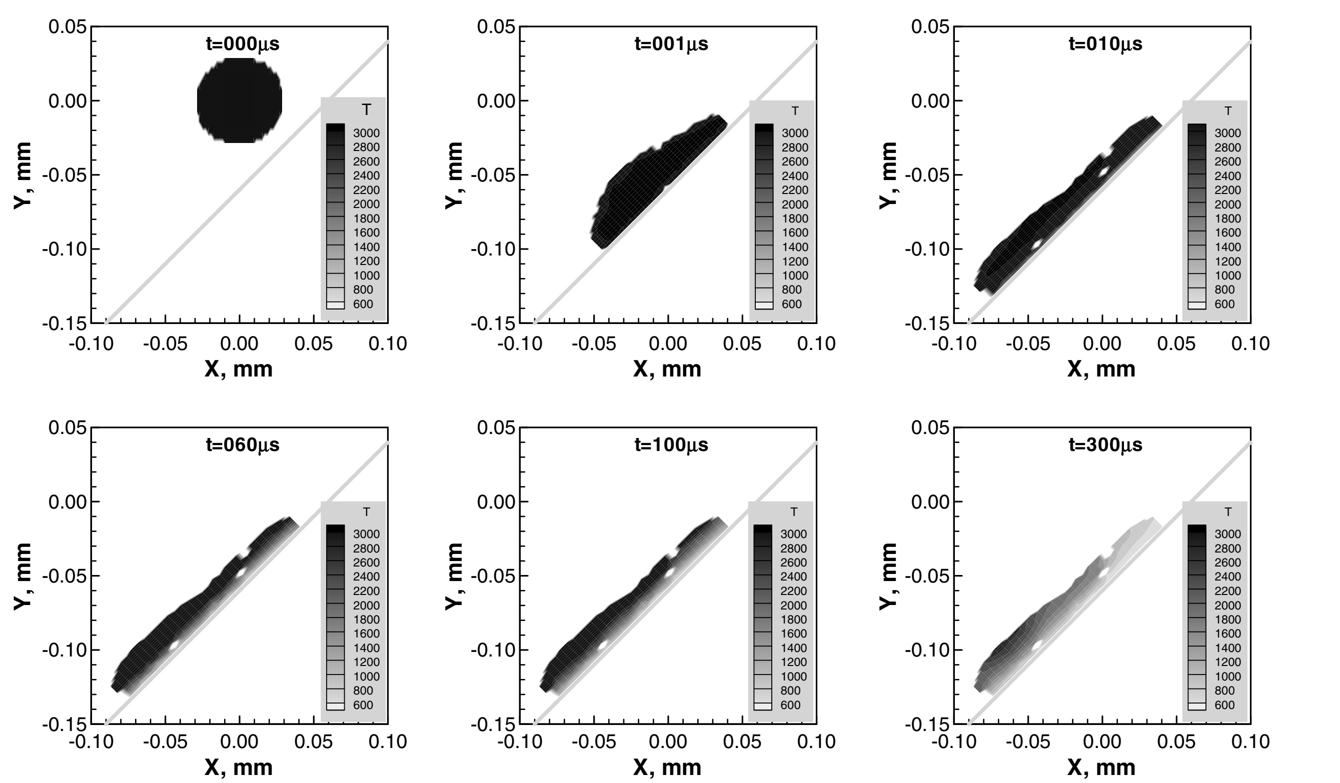

Fig. 5. Temperature distribution during 2D droplet impact on a cold substrate for $Re = 3535$ and impact angle of 45° with initial temperature of 3000 K.

$$K\begin{cases} < 3 & \text{rebound,} \\ \text{between} & \text{deposition,} \\ > 58 & \text{splashing.} \end{cases} \tag{17}$$

In regards to the above criterion, the droplet splashing occurs when the impact angle

$$\theta < \arccos(25.75\sigma^{2/5}\mu^{1/5}\rho^{-3/5}d^{-3/5}V^{-1}). \tag{18}$$

Eq. (18) predicts the critical impact angle of 44° for the YSZ droplet impacting at 80 m/s. This value has been proved by SPH simulations. Fig. 2 shows the predictions of YSZ droplet impacting on the substrate at the impact angles of 0°, 10°, 15°, 30°, and 40°, showing that all droplets splash. When droplets impact on the substrate at larger angle, e.g. 45°, 60°, and 75°, droplets deposit on the substrate as shown in Fig. 3. The splashing behavior has been summarized in Table 2. The simulation results agree well with the analytical prediction. The droplet splashing occurs when the impact angle is less than the critical impact angle of 44°. The droplet deposits when the impact angle is greater than 44°.

3.2. Splat formation at impact angle 45°

Fig. 4 shows that 2D YSZ droplet impacts onto a cold substrate for $Re = 3535$ and impact angle of 45° with initial temperature of 3000 K. The simulation results revealed that once YSZ droplet reaches the cold substrate, the

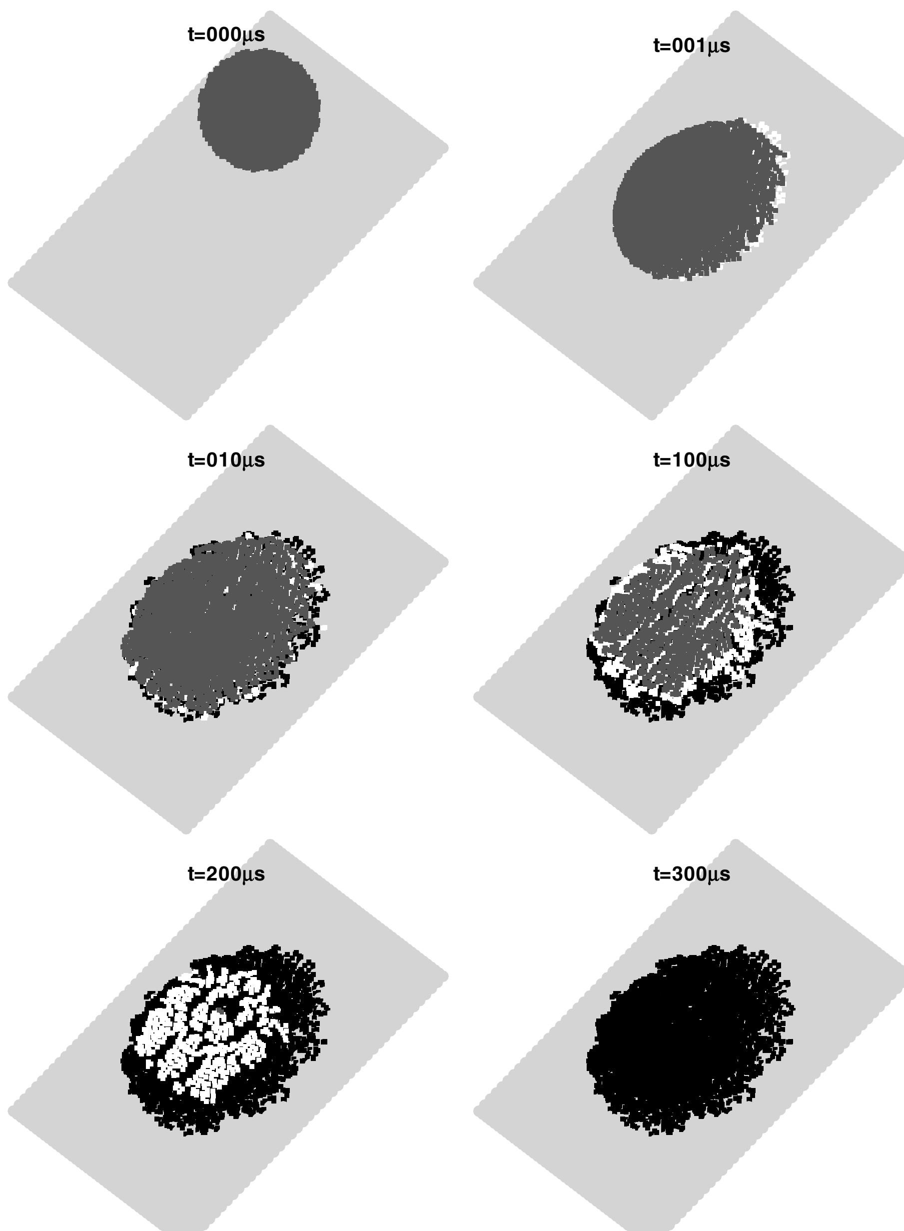

Fig. 6. 3D Droplet spreads on a cold substrate for $Re = 3535$ and impact angle of 45° with initial temperature of 3000 K. The dark gray color is liquid, the white color is the solidification interface, the dark color is solid, and the light gray color line is substrate.

droplet begins to deform and spread. At the same time, the solidification interface moves upwards and the droplet begins to solidify. At 1 μs, the liquid part of the splat deforms substantially. Initially, the solidification interface moves upwards quickly and captures many particles. After spreading is completed, the solidification interface moves slowly. This is due to the decrease of temperature gradient. At 10 μs, the droplet spreads substantially. At 300 μs, the droplet solidifies completely. There are voids entrapped into the splat.

Fig. 5 shows that the temperature distribution for 2D droplet impacting on a cold substrate at $Re = 3535$ and impact angle of 45° with initial temperature of 3000 K. As soon as the droplet with uniform initial temperature touches the cold substrate, the droplet temperature begins to decrease. At $t = 300$ μs, the temperature is higher at

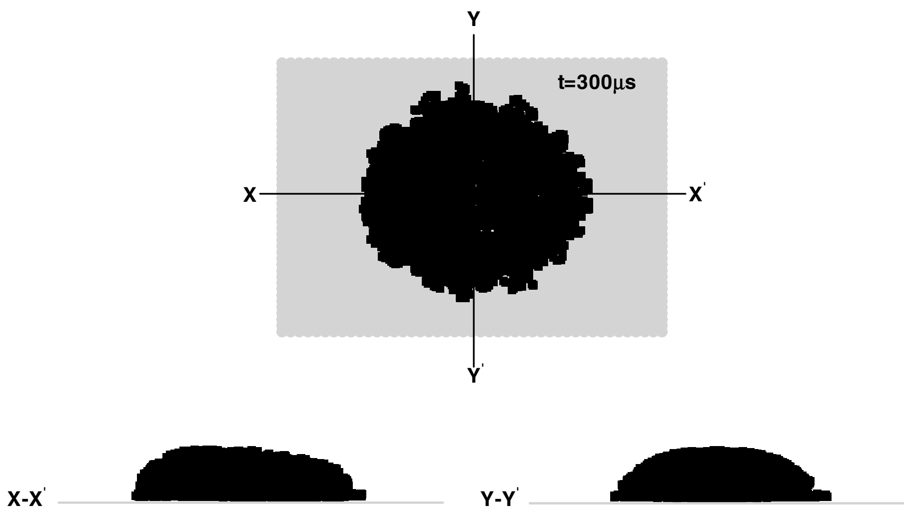

Fig. 7. The shape of the splat at $t = 300$ μs in the X–Y plane, X–X′, and Y–Y′ cross sections.

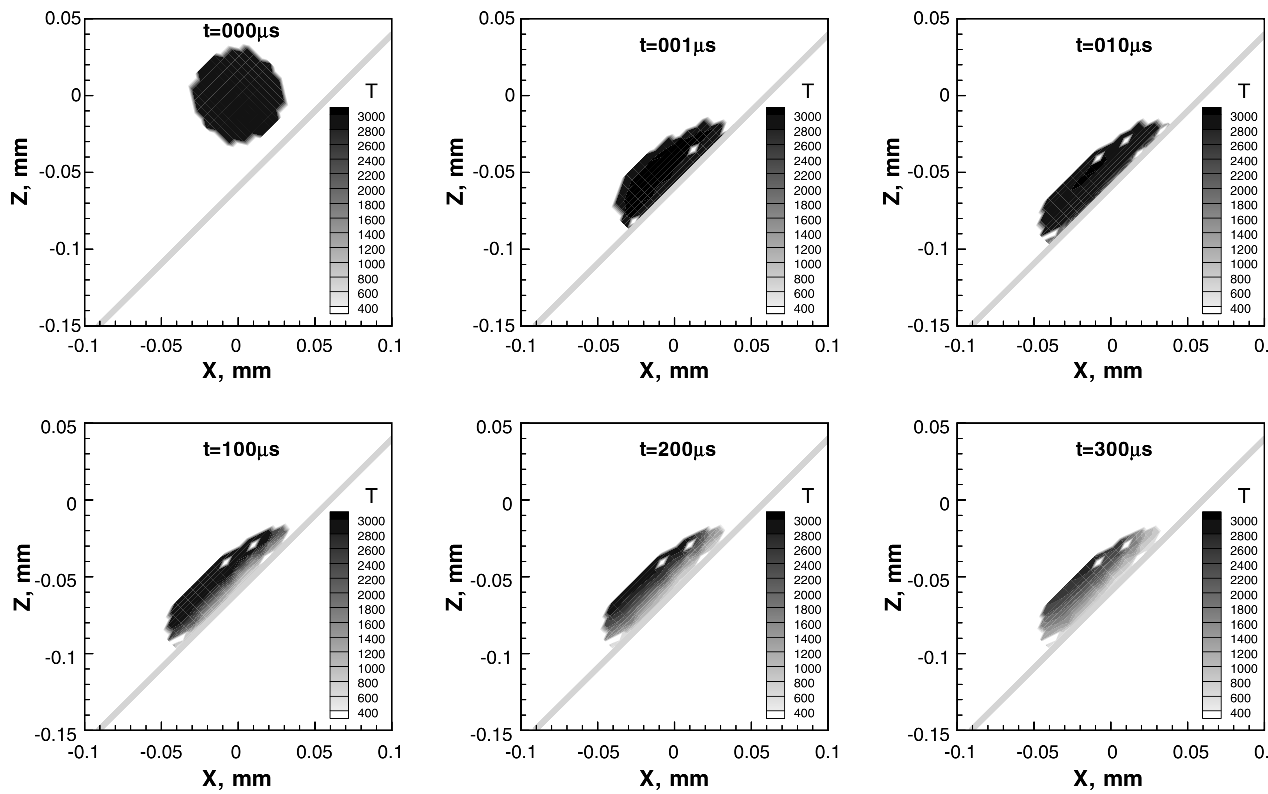

Fig. 8. Temperature distribution at the cross section $y = 0$ during 3D droplet impact on a cold substrate for $Re = 3535$ and impact angle of 45° with initial temperature of 3000 K.

the left top surface of the splat and the temperature is lower at the right top surface. The main reason is that the thickness of the splat is larger at the left end and the surface temperature needs more time to reduce. Since the thickness of the splat is lower at the right end, the surface temperature drops down faster.

Fig. 6 shows that 3D YSZ droplet impacts onto a cold substrate for $Re = 3535$ and impact angle of 45° with initial temperature of 3000 K. The results at 0, 1, 10, 100, 200, and 300 μs are provided. The initial temperature is close to the melting temperature. As soon as the droplet touches the cold substrate, the droplet begins to deform and solidify almost at the same time. The droplet deposits on the cold substrate. After the fast spreading of the droplet is completed, the droplet needs much time to complete solidification. The spherical droplet deforms to form a splat with the shape of a cylindrical disk.

Fig. 7 shows the shape of the splat at $t = 300\mu s$ in the X–Y plane, X–X', and Y–Y' cross sections. The shape of the splat in the X–X' cross section is not symmetric, because the impact velocity is not perpendicular to the substrate, while the shape of the splat in the Y–Y' cross section is almost symmetric. Fig. 8 shows that the temperature distribution at the cross section $y = 0$ for 3D droplet impacting on a cold substrate with $Re = 3535$, impact angle of 45° and initial temperature of 3000 K. As soon as the droplet impacts on the cold substrate, the droplet begins to cool down. Also there exists void formation during flattening.

3.3. Flattening ratio

The spreading behavior is characterized by the splat-flattening ratio ξ, which is defined as the ratio of the effective diameter of the splat to the droplet diameter

$$\xi = D/d_p, \tag{19}$$

where D is the effective diameter of the splat and d_p is the impacting droplet diameter. According to the theory [1,22], the flattening ratio can be expressed as a function of the particle Reynolds number as below [1]

$$\xi = CRe^{\alpha}, \tag{20}$$

where C takes the value of 1.2941 for a disk-shaped splat and the value of α can be either 0.2 or 0.125 or 0.167. Since the normal Reynolds number decreases with the impact angle, it will result in the decrease of the flattening ratio. However, the simulation results in Fig. 9 revealed that the spreading velocity increases with the impact angle; it helps the droplet spread when the impact angle is large. This is consistent with the theory by Zhang [7] where the role of the solidification is considered during flattening. It

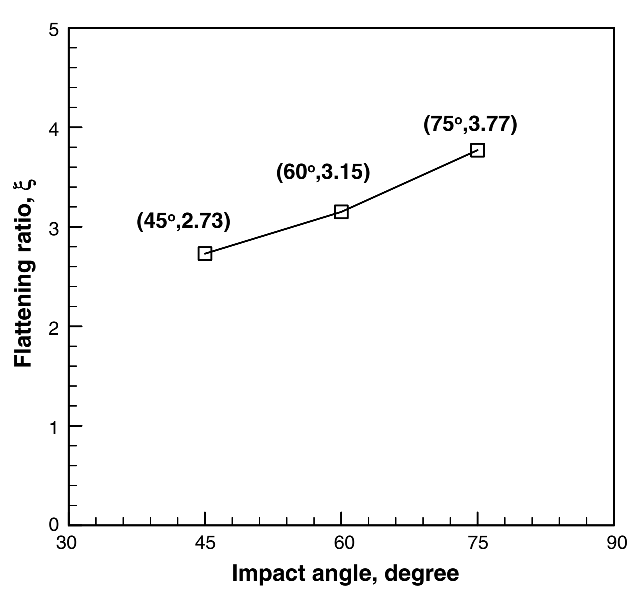

Fig. 9. The flattening ratio at the impact angles of 45°, 60°, and 75°.

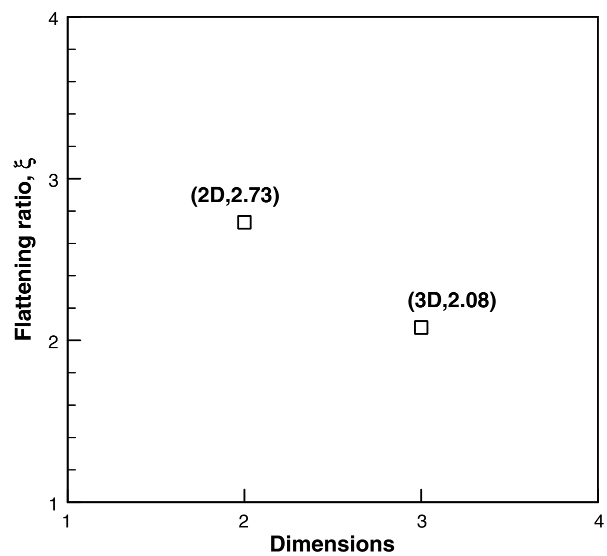

Fig. 10. The flattening ratio at the impact angle of 45° in 2D and 3D.

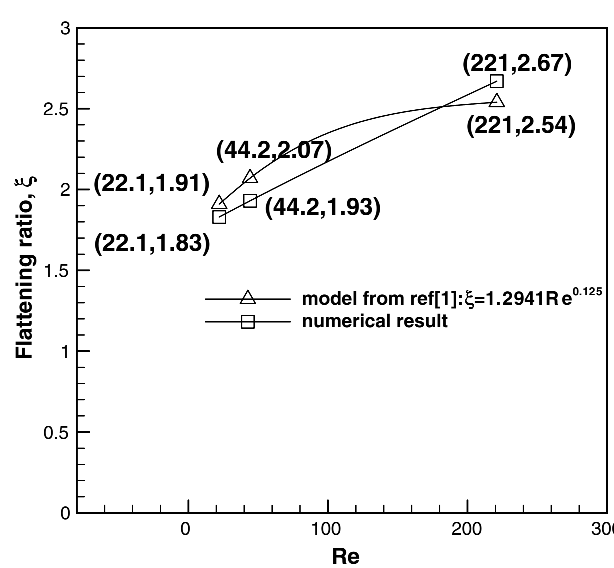

Fig. 11. The flattening ratio at different impact velocities during perpendicular impact.

is also found that the solidification effect exceeds the impacting kinetics. This confirms that it is necessary to consider the solidification effect when accounting for spreading. The flattening ratio at the impact angle of 45° in 2D and 3D are shown in Fig. 10. Due to surface tension, it is easier for a 2D cylinder to spread than for a 3D sphere. The aspect ratio of the splat is 1.39, which is defined as the ratio of major to minor diameter [5]. Fig. 11 shows the result from the above equation with $\alpha = 0.125$ and the numerical result at different impact velocities during perpendicular impact. The numerical result agrees well with the theory.

4. Conclusion

The SPH method has been applied to simulate the impact of YSZ droplet onto an inclined substrate where a small size of the droplet is used and surface tension is important. The surface tension is simulated based on the Lennard-Jones potential. Droplet impacting on an inclined substrate with different impact angles is investigated. When the impact angle is less than 44°, the droplet splashing occurs. It agrees well that the Sommerfeld number $K > 58$ induced splashing. The artificial heat model is improved and the temperature distribution is presented for a 3D droplet impacting on an inclined surface with the impact angle of 45°. Temperature drops down quickly at the thin end and slowly at the thick end. The flattening ratio is proportional to the impact angle, which is different from the theoretical prediction by the traditional theory of Madejski. Numerical simulations also prove that the meshless method, SPH, can be used to study droplet spreading, splashing and solidification very efficiently.

In the plasma spray experiments, substrate conditions are much more complicated. The splashing is commonly related to surface absorbates and wetting behavior changing with substrate temperature [23]. In the current simulations, we assumed that the substrate conditions are constant and do not change with time. Furthermore, equilibrium solidification is considered in the model instead of rapid solidification in the plasma spray experiments. Furthermore the gas phase is not included in the modeling. The conclusions are therefore limited to the assumptions used in the paper. However, the model developed in this paper is capable of including more complicated physics and dealing with splashing. In this paper, we have demonstrated the capability of the SPH method to solve droplet splashing, splashing and solidification problems which are difficult to handle by other meshed methods.

Acknowledgement

This work is financially supported by NSF CBET-0650604.

References

[1] P. Fauchais, M. Fukumoto, A. Vardelle, M. Vardelle, Knowledge concerning splat formation: an invited review, J. Therm. Spray Technol. 13 (3) (2004) 337–360.
[2] J. Mostaghimi, M. Pasandideh-Fard, S. Chandra, Dynamics of splat formation in plasma spray coating process, Plasma Chem. Plasma Process. 22 (1) (2002) 59–84.
[3] C. Escure, M. Vardelle, P. Fauchais, Experimental and theoretical study of the impact of alumina droplets on cold and hot substrates, Plasma Chem. Plasma Process. 23 (2) (2003) 185–221.
[4] S. Šikalo, C. Tropea, E.N. Ganic, Impact of droplets onto inclined surfaces, J. Colloid Interf. Sci. 286 (2) (2005) 661–669.
[5] C.W. Kang, H.W. Ng, Splat morphology and spreading behavior due to oblique impact of droplets onto substrates in plasma spray coating process, Surf. Coat. Technol. 200 (18–19) (2006) 5462–5477.
[6] L. Xu, W.W. Zhang, S.R. Nagel, Drop splashing on a dry smooth surface, Phys. Rev. Lett. 94 (18) (2005).
[7] H. Zhang, Theoretical analysis of spreading and solidification of molten droplet during thermal spray deposition, Int. J. Heat Mass Transfer 42 (14) (1999) 2499–2508.
[8] H. Zhang, X.Y. Wang, L.L. Zheng, X.Y. Jiang, Studies of splat morphology and rapid solidification during thermal spraying, Int. J. Heat Mass Transfer 44 (24) (2001) 4579–4592.
[9] H. Zhang, X.Y. Wang, L.L. Zheng, S. Sampath, Numerical simulation of nucleation, solidification and microstructure formation in thermal spraying, Int. J. Heat Mass Transfer 47 (2004) 2191–2203.
[10] H. Zhang, L.L. Zheng, V. Prasad, T.Y. Hou, A curvilinear level set formulation for highly deformable free surface problems with application to solidification, Numer. Heat Transfer Part B 34 (1998) 1–20.
[11] L.L. Zheng, H. Zhang, An adaptive level set method for moving-boundary problems: applications to droplet spreading and solidification, Numer. Heat Transfer Part B 37 (2000) 435–454.
[12] M. Bussmann, J. Mostaghimi, S. Chandra, On a three-dimensional volume tracking model of droplet impact, Phys. Fluids 11 (6) (1999) 1406–1417.
[13] M. Bussmann, S. Chandra, J. Mostaghimi, Modeling the splash of a droplet impacting a solid surface, Phys. Fluids 12 (12) (2000) 3121–3132.
[14] M. Pasandideh-Fard, S. Chandra, J. Mostaghimi, A three-dimensional model of droplet impact and solidification, Int. J. Heat Mass Transfer 45 (11) (2002) 2229–2242.
[15] M.Y. Zhang, H. Zhang, L.L. Zheng, Application of smoothed particle hydrodynamics method on free surface and solidification problems, Numer. Heat Transfer Part A: Appl. 52 (4) (2007) 299–314.
[16] R.B. Bird, W.E. Stewart, E.N. Lightfoot, Transport Phenomena, John Wiley & Sons, New York, 1960.
[17] D.A. Fulk, A Numerical Analysis of Smoothed Particle Hydrodynamics, Air Force Institute of Technology, 1994.
[18] R.F. Allen, The role of surface tension in splashing, J. Colloid Interf. Sci. 51 (1975) 350–351.
[19] S.Q. Armster, Thermo-fluid mechanisms controlling droplet based materials processes, Int. Mater. Rev. 47 (4) (2002) 169–190.
[20] C. Mundo, M. Sommerfeld, C. Tropea, Droplet-wall collisions – experimental studies of the deformation and breakup process, Int. J. Multiphase Flow 21 (2) (1995) 151–173.
[21] C.D. Stow, M.G. Hadfield, An experimental investigation of fluid-flow resulting from the impact of a water drop with an unyielding dry surface, Proc. Royal Soc. London Ser. A – Math. Phys. Eng. Sci. 373 (1755) (1981) 419–441.
[22] J. Madejski, Solidification of droplets on a cold surface, Int. J. Heat Mass Transfer 19 (1976) 1009–1013.
[23] S. Sampath, X. Jiang, Splat formation and microstructure development during plasma spraying: deposition temperature effects, Mater. Sci. Eng. A 304–306 (2001) 144–150.